Available online at www.sciencedirect.com
ScienceDirect
Applied Surface Science 254 (2008) 4688–4694
applied surface science
www.elsevier.com/locate/apsusc

Cobalt sorption properties of MgO prepared by solution combustion

F. Granados-Correa [a,*], J. Bonifacio-Martínez [a], V.H. Lara [b], P. Bosch [c], S. Bulbulian [d]

[a] Instituto Nacional de Investigaciones Nucleares, A.P. 18-1027, C.P. 11801 México, D.F., Mexico
[b] Universidad Autónoma Metropolitana, Iztapalapa, A.P. 55-532, Av. San Rafael Atlixco No. 186 Col. Vicentina, C.P. 09340 México, D.F., Mexico
[c] Instituto de Investigaciones en Materiales, Universidad Nacional Autónoma de México, A.P. 70-360, C.P. 04510 México, D.F., Mexico
[d] Centro de Ciencias Aplicadas y Desarrollo Tecnológico, Universidad Nacional Autónoma de México, A.P. 70-186, C.P. 04510 México, D.F., Mexico

Received 23 October 2007; received in revised form 14 January 2008; accepted 16 January 2008
Available online 24 January 2008

Abstract

Water effect on the combustion preparation of MgO is presented. The obtained materials are characterized through their specific surface area, morphology, particle shape, fractal dimension and Co^{2+} sorption. The surface fractal dimension of the combustion prepared sample was 2.0 but in those where water was included it decreased to 1.8. In the sample prepared by calcination it was 2.3. A linear correlation between the fractal dimension and Co^{2+} sorption was found.

Keywords: Magnesium oxide; Solution combustion method; Surface properties; Fractal dimension; Cobalt sorption

1. Introduction

Many oxides possess some catalytic activity for oxidative dimerization of methane, among them is magnesium oxide. The addition of alkali metals improves their activity and selectivity; for instance, on Li-promoted MgO the products are ethane, ethene and CO [1]. Magnesia has been synthesized from hydrotalcite to obtain compounds with a pronounced basic character very active in the double-bond isomerization of 1-pentane [2].

Magnesium oxide adopts periclase structure and has very high lattice energy (3938 kJ/mol). Magnesia is a compound that may be synthesized by precipitation or sol–gel methods [3]. The rapid combustion synthesis of MgO stabilized with Sr has been already published [4]. However, the synthesis of pure MgO by the solution combustion method has not been reported. Combustion synthesis technique requires the use of an organic compound, like urea, which, reacting with oxygen, heats the initial salts. In this sense, it is economical and fast, but it may issue in new morphologies or even different compounds than those provided by precipitation [5]. Solution combustion synthesis has also been used to produce oxides with large surface areas [6].

The control of the very exothermal urea combustion is essential. For instance, porous materials with a hierarchical texture as SiO_2 [7,8] or Al_2O_3 [9] present nanopores, which are determining in their applications. The surface area or the pore size distributions are, with morphology, some of the parameters that condition reactivity, electrochemical and catalytic activities, and molecular sieve effect. As the main differences between conventional oxides and combustion prepared materials have to be textural, their surface adsorption properties have to be different.

In this work we present the solution combustion synthesis of MgO and we compare the morphology of the obtained compounds varying several synthesis parameters with the corresponding sample synthesized by calcination of magnesium nitrate. To test these surface structure variations, the cobalt sorption, often found in wastewaters from nuclear industry, may be used. Indeed, cobalt retention is, now, well understood [10–13].

2. Experimental

2.1. Materials

The following analytic grade materials were used without further purification: Urea NH_2CONH_2 A.C.S. reagent (Sigma–Aldrich, 99–100 wt% purity), magnesium nitrate hexahydrate

* Corresponding author. Tel.: +55 53297200; fax: +55 53297301.
E-mail address: fgc@nuclear.inin.mx (F. Granados-Correa).

0169-4332/$ – see front matter © 2008 Elsevier B.V. All rights reserved.
doi:10.1016/j.apsusc.2008.01.074

$Mg(NO_3)_2{\cdot}6H_2O$ A.C.S. reagent (Sigma–Aldrich, 99 wt% purity), cobalt nitrate hexahydrate $Co(NO_3)_2{\cdot}6H_2O$ reagent (Baker, 100.7 wt% purity) and potassium bromide KBr (Madison Co. spectroscopy grade).

2.2. Synthesis by solution combustion method

Magnesium oxide powder was prepared with 0.2 g of $Mg(NO_3)_2{\cdot}6H_2O$ and 0.4 g of urea mixed and suspended in 1 mL of distilled water until a homogeneous solution was obtained. The mixture was heated until most of the water evaporated with the help of an electric grill, resulting in a humid integrated solid. Six more samples were prepared diluting this fraction in 0.5, 1, 1.5, 2, 2.5 and 3 mL of water. These mixtures were transferred into 30 mL crucibles, which were introduced for 5 min into a muffle furnace. Heating temperature was 800 °C.

2.3. Synthesis by calcination method

0.2 g of $Mg(NO_3)_2{\cdot}6H_2O$ were transferred into a 30 mL crucible, which was introduced for 2 h into a muffle furnace. Again, heating temperature was 800 °C.

2.4. Characterization

A Siemens D-5000 diffractometer coupled to a copper anode tube was used to obtain the X-ray diffraction patterns and identify the crystalline compounds. The K_α wavelength was selected with a diffracted beam monochromator.

To be sure that no organic radicals due to urea combustion remained, infrared experiments were performed. A spectrophotometer Nicolet 550 was used and the samples were mixed to KBr in the conventional way.

Radial distribution functions were calculated from X-ray diffraction patterns obtained using a molybdenum anode X-ray tube coupled to a Siemens D500 diffractometer. The required high values of the angular parameter were, in this way, reached. The K_α radiation was selected with a filter and the data, measured by step scanning with a scintillation counter, were the input to the Radiale program [14].

A Kratky camera coupled to a copper anode tube was used to measure the small angle X-ray scattering (SAXS) curves. The distance between the sample and the linear proportional counter was 25 cm; a Ni filter selected the copper K_α radiation. The sample was introduced into a capillary tube. Intensity $I(h)$ was measured for 9 min in order to obtain good quality statistics. The SAXS data were processed with the ITP program [15,16] where the angular parameter (h) is defined as $h = 2\pi\sin\theta/\lambda$, where θ and λ are the X-ray scattering angle and the wavelength, respectively. The shape of the scattering objects was estimated from the Kratky plot, i.e., $h^2I(h)$ versus h. The shape is determined depending on the Kratky curve shape; then, for instance, if the curve presents a peak the particles are globular (bubbles) [17]. If a shape can be assumed, the size distribution function may be calculated. Finally, it is often useful to estimate, from the slope of the curve $\log I(h)$ versus $\log(h)$, the fractal dimension of the scattering objects [18,19]. For this study the background obtained with the Porod plot was removed from the experimental intensity. The h interval was $0.07 < h < 0.18$ Å^{-1}. Note that, by the Babinet principle, the SAXS may be either due to dense particles in a low-density environment or pores – or low-density inclusions – in a continuous high-electron-density medium. Therefore, in this work we will use the word ''heterogeneity'' to design the scattering objects that may be pores or particles.

Morphology was determined using a scanning electron microscope (SEM) Philips XL-30 and specific surface areas were obtained by nitrogen adsorption through the BET method with a surface area analyzer Micromeritics Gemini 2360. In order to give a coherent picture of the most important characteristics the surface fractal dimension was also determined from the nitrogen adsorption isotherms according to the equation proposed by Pfeifer and Cole [20]:

$$\ln\left(\frac{V}{V_m}\right) = \text{constant} + \frac{(D-3)}{3}\left\{\ln\left[\ln\left(\frac{p_0}{p}\right)\right]\right\} \quad (1)$$

This equation relates the multilayer coverage of the surface to the relative pressure, p_0/p, where V is the adsorbed gas volume and V_m is the volume of monolayer both at standard temperature and pressure; p is the equilibrium pressure and p_0 is the saturation pressure. If $\ln(V/V_m)$ is plotted as a function of $\ln[\ln(p_0/p)]$, a straight line should be obtained whose slope should be proportional to the surface fractal dimension D. This analysis is valid in the range $-1.6 < \ln[\ln(p_0/p)] < 1.2$. The correlation between the experimental data and the straight line is given by a correlation factor R^2.

2.5. Cobalt sorption

Batch experiments were carried out at room temperature mixing, in closed vials, 0.1 g of each MgO and 10 mL of $^{60}Co^{2+}$ solution at pH of 5.5. Samples were stirred for 10 s and shaken for 1 h. The liquids were separated from the solids by centrifugation (5 min at 3000 rpm). The radioactivity of $^{60}Co^{2+}$ in each aliquot of 5 mL was measured with an Ortec Ge/hyperpure solid state detector coupled to a multichannel analyzer (4096 channels) previously calibrated with ^{204}Tl (71 keV), ^{22}Na (511 and 1274 keV) and ^{137}Cs (662 keV) radioactive sources: the activity of $^{60}Co^{2+}$ was calculated from the 1173 and 1332 keV peaks by means of a suitable computer program (Teacher) in the multichannel analyzer. Radioactive $^{60}Co^{2+}$ was obtained by thermal neutron irradiation of a specific solution of $Co(NO_3)_2{\cdot}6H_2O$ for 1 h in the Triga Mark III nuclear reactor at the Centro Nuclear de México, with a neutron flux of 10^{12}–10^{13} n cm^{-2} s^{-1}.

3. Results

3.1. Compound identification

In Fig. 1, the X-ray diffraction patterns of the samples prepared by combustion are compared to the pattern of the

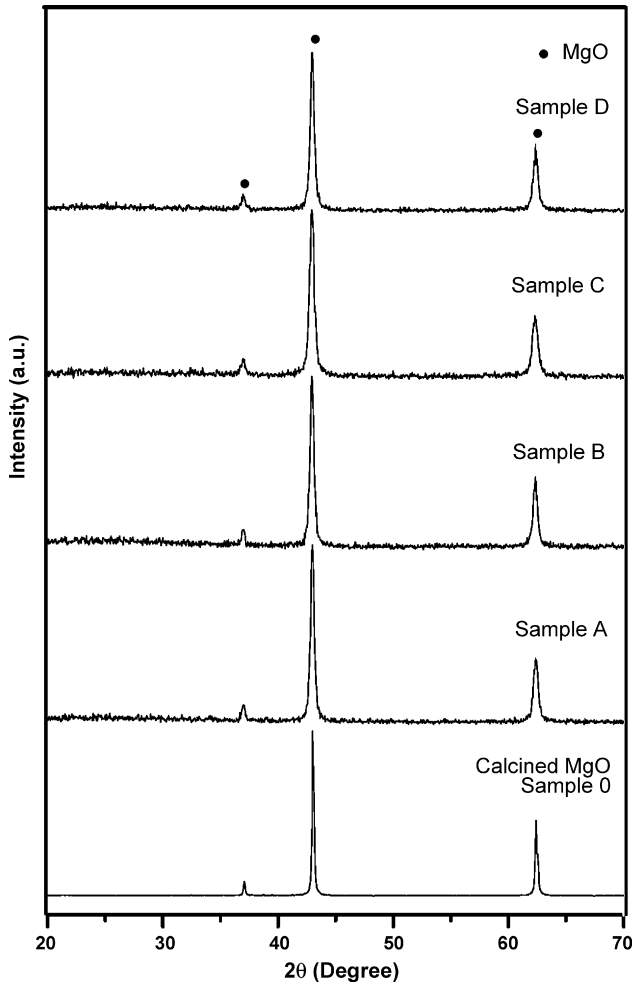

Fig. 1. X-ray diffraction patterns of the samples prepared by (0) calcination of magnesium nitrate, (A) by combustion MgO (B) by solution combustion MgO-$1H_2O$ (C) MgO-$2H_2O$ and (D) MgO-$3H_2O$.

MgO prepared by calcination of magnesium nitrate. The sharp and well-defined peaks, present in all samples, correspond to MgO (periclase). A broad peak centered at ca. 25° reveals, in the combustion and solution combustion prepared samples, the presence of a non-crystalline phase. Hence, all the synthesized materials are constituted by crystalline periclase (MgO) and a fraction of non-crystalline compound, only the sample 0 prepared by calcination of magnesium nitrate was fully crystalline, Table 1. The infrared spectra did not show any band attributable to organic residues.

3.2. Radial distribution functions

To characterize the non-crystalline fraction, the radial distribution functions were calculated as they provide the interatomic distances in the short-range order. Fig. 2 shows that, in this sense, all samples are similar, therefore the radial atomic structure, for a radius comprised between 1 and 10 Å, is the same, and the non-crystalline material presents the same short-range order as the crystalline MgO, otherwise different atomic distances would appear or, at least, peaks would be shifted, Table 2.

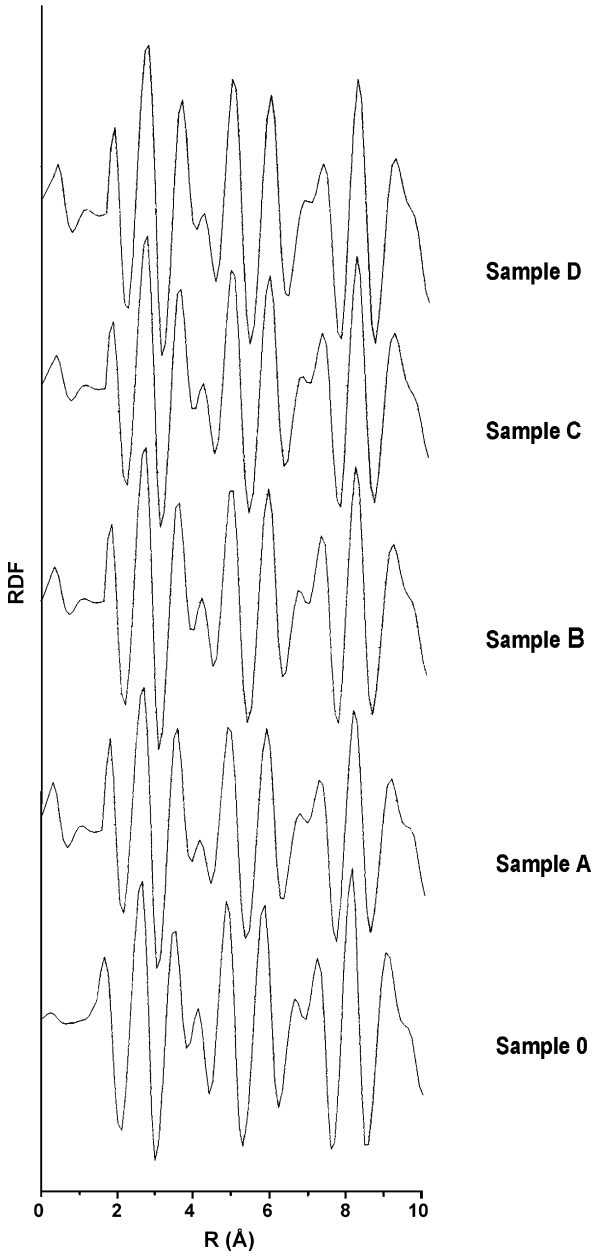

Fig. 2. Radial distribution functions (RDF) of the prepared samples.

3.3. Small angle X-ray scattering (SAXS)

The Kratky plots are shown in Fig. 3. Only the MgO prepared by calcination shows the typical peak of globular particles. The dried and combustion prepared materials present a lamellar morphology. Assuming such morphologies, the heterogeneity size distributions were obtained, Fig. 4. The maxima in the calcined MgO correspond to radii of 45, 70 and 100 Å; most particles are 100 Å. These values are much larger than those obtained for the other prepared materials whose heterogeneity size distributions presented a broad peak for small heterogeneities and a well-resolved peak for a radius of 70 Å.

The fractal dimension, obtained from SAXS experiments, Table 2, follows the same pattern as the highest value is found

Table 1
Compounds identified by XRD in each sample and BET surface areas

Sample	Synthesis	Treatment	Compounds	Surface area (m^2/g)
0	Calcined MgO	Calcination	MgO (periclase)	1.7
A	Combustion synthesis	Combustion	MgO (periclase) + non-crystalline	28.0
B	MgO-H_2O (1 mL)	Solution combustion	MgO (periclase) + non-crystalline	52.0
C	MgO-H_2O (2 mL)	Solution combustion	MgO (periclase) + non-crystalline	51.0
D	MgO-H_2O (3 mL)	Solution combustion	MgO (periclase) + non-crystalline	45.0

Table 2
Comparison of the results determined by SAXS, SEM and BET

Sample	Radial distribution function (XRD)	Shape of heterogeneities (SAXS)	Fractal dimension (SAXS)	Pore size distribution, maxima in Å (SAXS)	Particle morphology (SAXS)	Surface fractal dimension (BET) R^2
0	MgO structure only	Spheres	3.0	45, 70, 100	No defined morphology	2.0 ($R^2 = 0.9616$)
A combustion synthesis	MgO structure only	Lamellae	2.3	Broad, 70	Homogeneous, small particles (ca. 0.1 μm)	1.8 ($R^2 = 0.9967$)
B (1 mL)	MgO structure only	Lamellae	2.3	Broad, 70	Large bubbles, lamellar	1.7 ($R^2 = 0.9968$)
C (2 mL)	MgO structure only	Lamellae	2.3	Broad, 70	Bubbles, slightly more compact, lamellar	1.7 ($R^2 = 0.9988$)
D (3 mL)	MgO structure only	Lamellae	2.3–2.5	Broad, 70	Much more compact, some particles ca. 0.1 μm	1.7 ($R^2 = 0.9973$)

for the precipitated and calcined sample, which does not present a fractal structure. The combustion (sample A) and the solution combustion prepared magnesias (samples B–D) are the more fractally structured oxides (2.3), instead sample 0 has a fractal dimension of 3.0. These values are volume fractal dimensions and show that the connectivity of the magnesia structure depends on the preparation method. They will be interpreted in Section 4, in terms of the surface fractal dimensions obtained by nitrogen adsorption.

3.4. Scanning electron microscopy (SEM)

The size and shape of the grains of the synthesized MgO determined by SEM are very different. The particles of the calcined sample are so large that no texture is observed. The surface is smooth and typical of a well-crystallized material. The combustion prepared MgO presents homogeneous particles whose size is close to 0.1 μm. The combustion prepared materials with 1 and 2 mL present a clear lamellar structure and large ''craters'' can be observed. The 2 mL sample seems to be denser than the 1 mL. The combustion prepared MgO (3 mL) sample is much more compact although some small particles (0.1 μm) are observed, Fig. 5.

3.5. BET specific surface area

The specific surface area of calcined MgO turned out to be 1.7 m^2/g, instead all other samples presented areas comprised between 28 and 52 m^2/g. The highest value was 52 m^2/g obtained for the MgO prepared by combustion with 1 mL of water. A variation of 1 mL of water (from 2 to 3 mL) diminishes the surface area in more than 25%; therefore, the control of combustion reaction through water is essential to obtain high specific surface areas. Fig. 6 correlates the specific surface area of MgO samples obtained by combustion with the water amount added during synthesis.

When the surface fractal dimension was obtained from N_2 adsorption data, the values were, for calcined MgO (sample 0), 2.0 and 1.8 for the combustion prepared sample. For the solution combustion samples, B, C and D, the value was 1.7, Table 2 and Fig. 7.

3.6. Cobalt retention

The amount of retained cobalt ion is shown in Fig. 8. The value for MgO obtained by calcination (sample 0) was 2.1%, but for MgO obtained by combustion (sample A) it was 25.0%. The percentage increased up to 32.5% (sample B) but it decreased slightly to 32.0% and 29.0% for samples C and D, respectively.

4. Discussion

The surface area values follow the same trend as those reported by Mimani and Patil [6] for ZrO_2. Indeed, the surface area of the solution combustion prepared MgO is larger than that of combustion or calcined samples. Results seem to be contradictory, indeed, on the contrary, the combustion samples present some non-crystalline material but the interatomic distances are the same as in the fully crystalline MgO. The SAXS heterogeneity size distributions show that the particles (or pores) are smaller than 100 Å but the smaller particles observed by SEM are 0.1 μm. Lastly the cobalt amount retained seems to be rather independent of the features of the prepared samples.

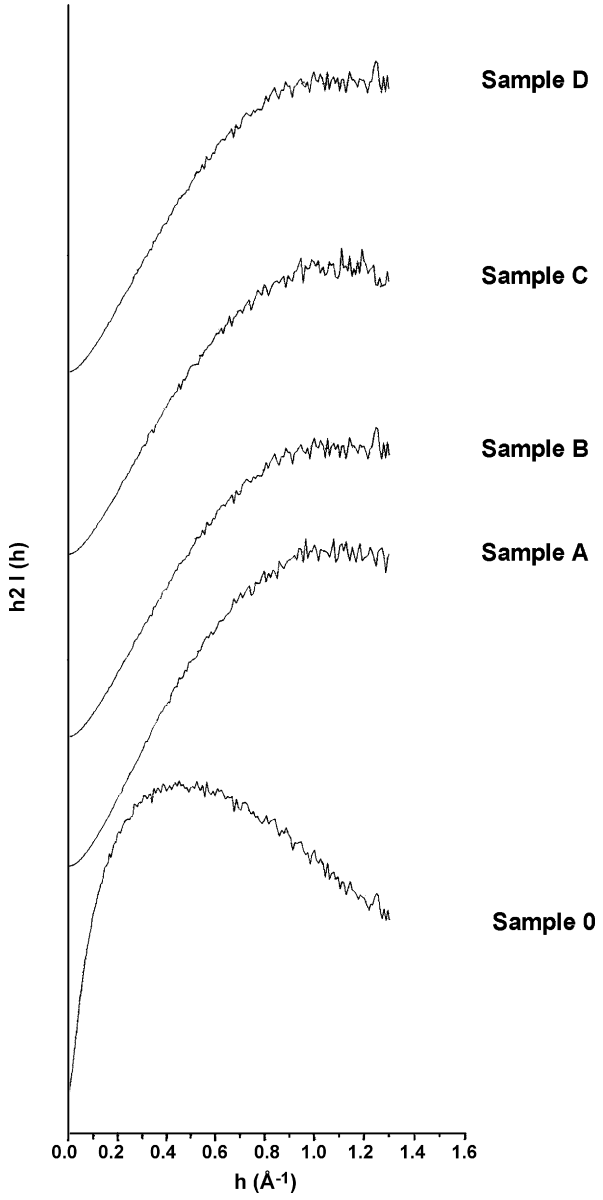

Fig. 3. Kratky plots of prepared samples determined by SAXS.

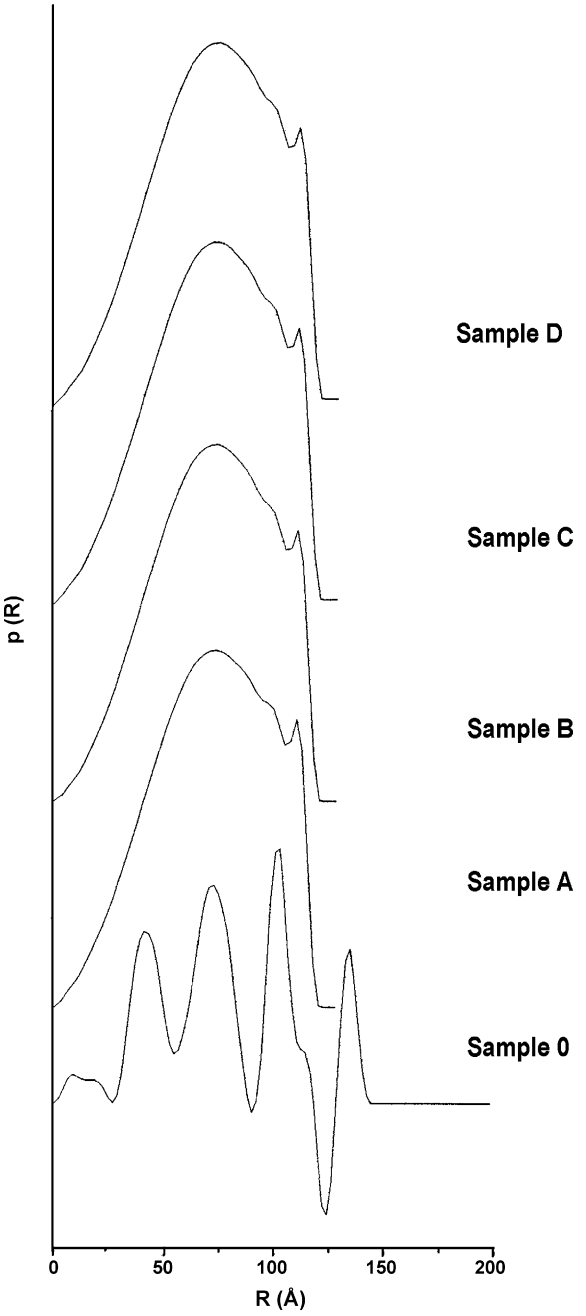

Fig. 4. Particle size distributions determined by SAXS.

The presence of a bump in the X-ray diffraction patterns of the combustion prepared samples whose structure, as determined by the radial distribution functions, corresponds to MgO may be understood if a bimodal particle size is accepted. Note that, if the crystallite size of a compound is around 30–70 Å or if a considerable strain is present between the planes, the corresponding peaks become broad. Such is the case in the combustion prepared materials. The combustion obtained MgO presents, both, large crystals and very small ones. Such conclusion is in agreement with the SAXS heterogeneity size distributions, which presents broad peaks centered at 60 Å and with the SEM micrographs that show sizes as large as 0.1 μm. Then, the heterogeneities observed in SAXS are particles with a lamellar morphology as shown by the Kratky plots and the SEM micrographs. The high specific surface areas are, then, due to those small particles.

Instead, sample 0 has only large globular particles as shown by SEM, SAXS and the very low surface area. The particle size distribution obtained by SAXS in this material is not representative as X-ray diffraction peaks are not broadened and the surface area is very small. Nevertheless, in this sample the SAXS size distribution could be interpreted as a pore size distribution.

The combustion prepared magnesia presents differences due to the water amount incorporated during synthesis. The micrographs of solution combustion samples show clear bubbles that explode forming craters and cavities on the surface. Such morphology reveals the presence of vapors that are liberated when the sample is viscous. In this sense, the

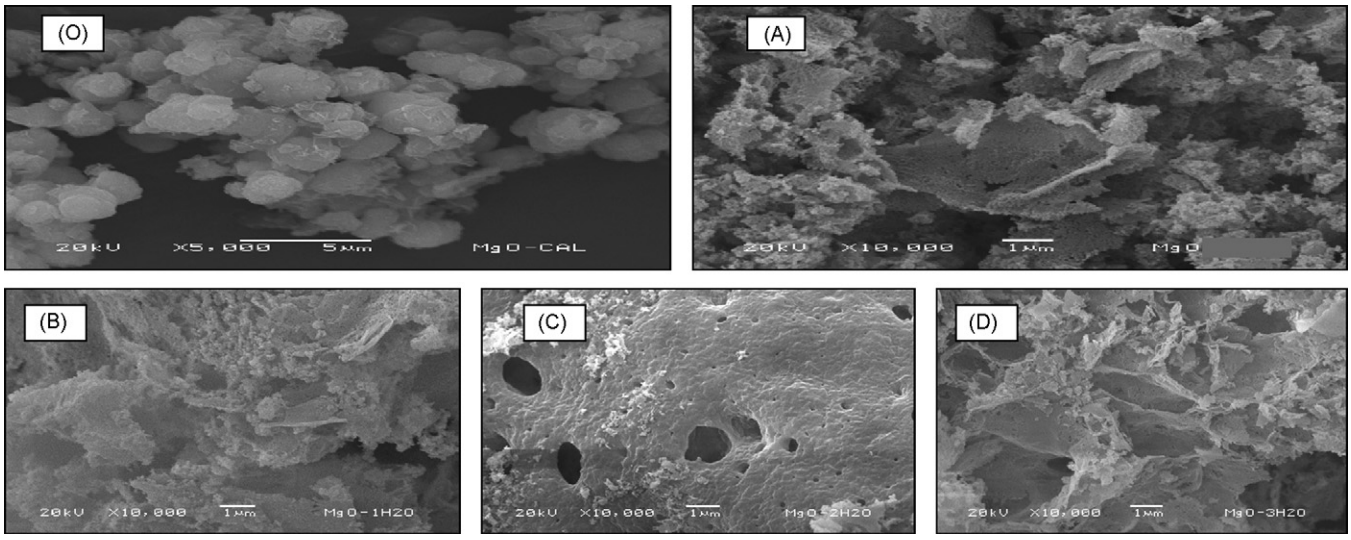

Fig. 5. Top-view SEM images of the MgO samples. (0) calcined MgO, (A) combustion MgO, (B) MgO-H_2O, (C) MgO-$2H_2O$, (D) MgO-$3H_2O$.

fractal dimension values determined by SAXS are relevant as they show that those materials (B–D) have a lower volume fractal dimension. The surface fractal dimension determined by BET reproduces this behavior as the combustion prepared samples in presence of water present the same surface fractal dimension value (1.7). If the fractal dimension is correlated to cobalt retention the curves are linear within error range, Fig. 9. In a previous work, the fractal dimension of irradiated cobalt zeolites was correlated with cobalt leaching in presence of a sodium chloride solution. A linear behavior was also observed, the highest the fractal dimension the lowest the leaching [10]. This study shows that such conclusion is valid. It has to be emphasized that cobalt retention is proportional to fractal dimension independently of the sorbent nature.

Such behavior may be compared with results reported for other lamellar compounds where fractal dimension is said to describe the degree of roughness and porosity of the surface; in silica the fractal dimension value is 2.01, but in montmorillonite and illiite it is 2.83 and 2.58, respectively. In kaolinite it is 2.12 [21]. In our solution combustion prepared samples, also a lamellar structure, the obtained volume fractal dimension was 2.3 and surface fractal dimension was 1.7; these values are, then, in the range of other lamellar materials and show that the surface structure as described by the surface fractal dimension is determined by the volume fractal dimension in this material.

The combustion preparation, samples A–D, apparently provides materials with a high sorption capacity if compared with the retention of the calcination prepared material, sample 0. Still, if the percentage of cobalt retained per m^2 is calculated, in the combustion prepared materials it varies if water is added: sample A retained 0.90, but samples B–D 0.63–0.65% Co^{2+}/m^2/g. The correlation with the fractal dimension is more relevant as it shows how the local structure of the surface determines the amount of cobalt retained. Again, the highest value is obtained for 0.5 and 1 mL of water.

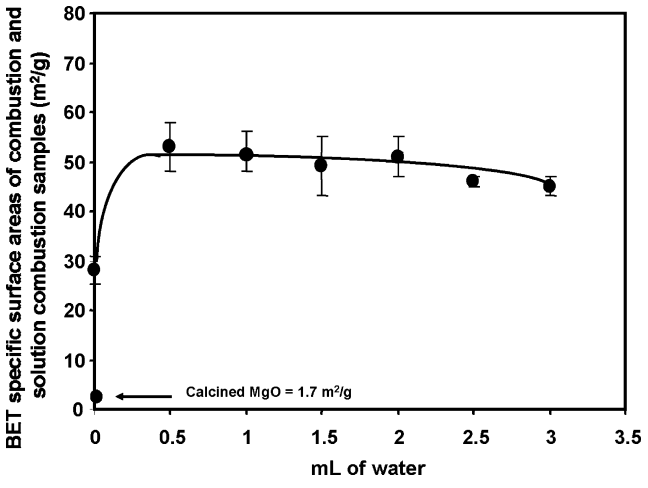

Fig. 6. BET specific surface areas of the combustion and solution combustion prepared samples as the function of water amount added during synthesis.

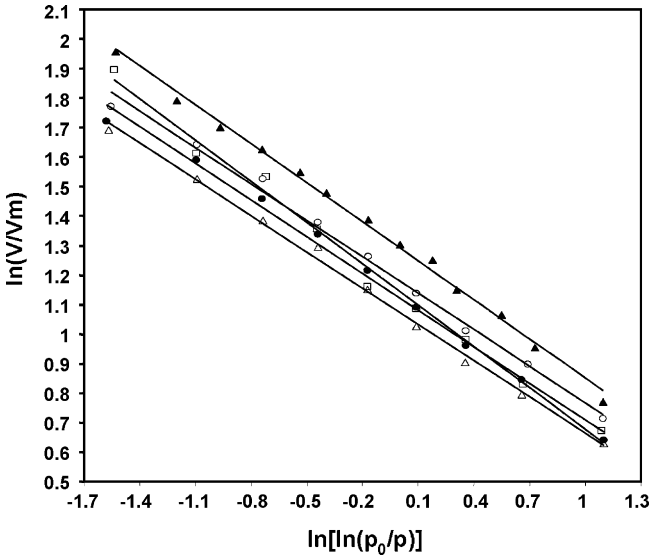

Fig. 7. $\ln(V/V_m)$ versus $\ln[\ln(p_0/p)]$ to determine the surface fractality: MgO-H_2O (open circles), MgO-$2H_2O$ (open triangles), MgO-$3H_2O$ (closed circles), calcined MgO (open charts), combustion MgO (closed triangles).

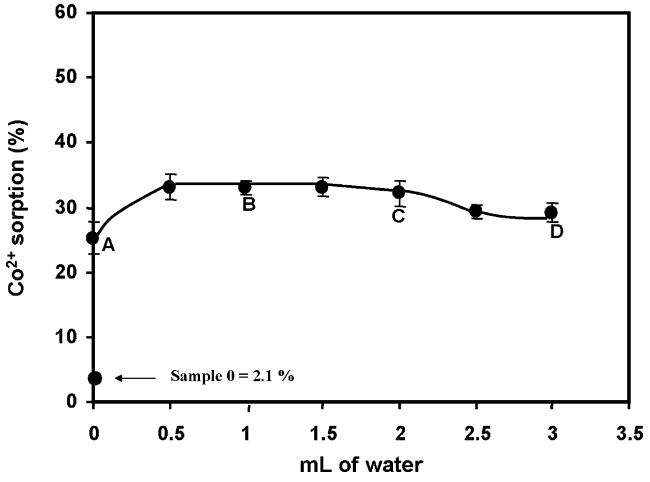

Fig. 8. Co^{2+} sorption on the combustion and solution combustion prepared samples. Experimental conditions: concentration of $Co^{2+} = 1.0 \times 10^{-4}$ M; pH 5.5, room temperature.

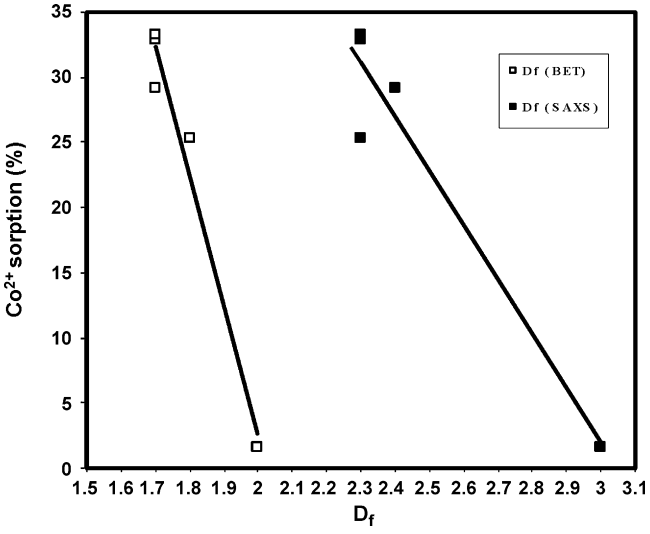

Fig. 9. Correlation Co^{2+} sorption in fractal dimension.

5. Conclusions

Magnesium oxide prepared by combustion method with urea presents a surface area of 28 m^2/g; this value is much higher than that obtained by calcination (1.7 m^2/g). The effect of incorporating water in the combustion synthesis of MgO provides materials with higher surface area, 45–52 m^2/g, and a higher capacity to retain Co^{2+}. The sample prepared by combustion with 0.5 or 1 mL of water retained the highest Co^{2+} amount (32%).

Cobalt sorption is correlated linearly with surface and volume fractal dimensions determined by BET and SAXS. Morphology depends on the amount of incorporated water; a lamellar structure and large "craters" can be observed. The 2 mL sample seems to be denser than the 1 mL. When the sample is prepared with 3 mL, it turns out to be much less compact although some small particles (0.1 μm) are observed.

Hence, the material prepared with 1 mL of water (surface area: 52 m^2/g, surface fractal dimension: 1.7, morphology: lamellar, particle size distribution: broad and centered in 70 Å) presented the best performance in Co^{2+} retention. Most probably, when more water is added, a fraction of the combustion heat is used to evaporate the excess water as shown by the craters observed in the SEM micrographs.

Acknowledgements

The authors are grateful to C. Rodriguez F. and E. Morales from ININ for technical help.

References

[1] C.H. Lin, K.D. Campbell, J.K. Wang, J.H. Lunsford, J. Phys. Chem. 90 (1985) 5062.
[2] H. Schaper, J.J. Berg-Slot, W.H. Stork, J. Appl. Catal. 54 (1989) 79.
[3] W.K. Hyoum, H.S. Seung, L. Chongmu, J. Korean Phys. Soc. 49 (2006) 628.
[4] T. Mathews, R. Subasri, O.M. Sreedharan, Solid State Ionics 148 (2002) 135.
[5] S. Martínez-Gallegos, H. Pfeiffer, E. Lima, M. Espinosa, P. Bosch, S. Bulbulian, Micropor. Mesopor. Mat. 94 (2006) 234.
[6] T. Mimani, K.C. Patil, Mater. Phys. Mech. 4 (2001) 134.
[7] P. Dieudonne, J.J. Phalippou, Sol-Gel Sci. Technol. 14 (1999) 249.
[8] E. Vinogradova, A. Moreno, V.H. Lara, P. Bosch, Silic. Chem. 2 (2003) 247.
[9] J.S. Valente, S. Falcon, E. Lima, M.A. Vera, P. Bosch, E. López-Salinas, Micropor. Mesopor. Mat. 94 (2006) 277.
[10] E.J. Lima, P. Bosch, V.H. Lara, S. Bulbulian, Chem. Mater. 16 (2004) 2255.
[11] A. Sampieri, G. Fetter, P. Bosch, S. Bulbulian, Langmuir 22 (2006) 385.
[12] R. Rodríguez-Trejo, P. Bosch, S. Bulbulian, Nucl. Mat. 354 (2006) 110.
[13] E. Lima, P. Bosch, S. Bulbulian, Appl. Radiat. Isot. 65 (2007) 259.
[14] M. Magini, A. Cabrini, J. Appl. Crystallogr. 29 (1972) 702.
[15] O. Glatter, J. Appl. Crystallogr. 21 (1988) 886.
[16] O. Glatter, K. Gruber, J. Appl. Crystallogr. 26 (1993) 512.
[17] M. Kataoka, J.M. Flanagan, F. Tokunaga, D.M. Engelman, Use of X-ray solution scattering for protein folding study, in: B. Chanse, J. Deisenhofer, S. Ebashi, D.T. Goodhead, H.E. Huxley (Eds.), Synchrotron Radiation in the Biosciences, vol. 4, Clarendon Press, Oxford, U.K., 1994, pp. 87–92.
[18] A. Harrison, Fractals in Chemistry, Oxford University Press Inc., New York, U.S.A., 1995.
[19] J.E. Martin, A.J. Hurd, J. Appl. Crystallogr. 20 (1987) 61.
[20] P. Pfeifer, M.W. Cole, New J. Chem. 12 (1990) 221.
[21] T. Pernyeszi, I. Dékány, Colloid Polym. Sci. 281 (2003) 73.